Acta Cryst. (1997). B53, 280–292

Structures of the Optically Active Monofluoro-Substituted Mandelic Acids: Relation to Their Racemic Counterparts and Thermochemical Properties

SINE LARSEN* AND KATALIN MARTHI

Centre for Crystallographic Studies,† Department of Chemistry, University of Copenhagen, Universitetsparken 5, DK-2100 Copenhagen, Denmark. E-mail: sine@xray.ki.ku.dk

(Received 8 July 1996; accepted 25 October 1996)

Abstract

The crystal structures of the three optically active monofluoro-substituted mandelic acids ($C_8H_7FO_3$, M_r = 170.14) have been determined from low-temperature X-ray diffraction data. (*R*)-(–)-*ortho*-Fluoromandelic acid, monoclinic, $P2_1$, a = 8.356 (2), b = 10.842 (2), c = 8.544 (2) Å, β = 94.13 (2)°, Z = 4, m.p. 361.8 (5) K. (*R*)-(–)-*meta*-Fluoromandelic acid, monoclinic, $P2_1$, a = 8.493 (3), b = 5.8426 (7), c = 15.628 (3) Å, β = 104.10 (2)°, Z = 4, m.p. 394.2 (5) K. (*R*)-(–)-*para*-Fluoromandelic acid, monoclinic, $C2$, a = 8.464 (2), b = 5.8518 (13), c = 15.868 (2) Å, β = 107.56 (2)°, Z = 4, m.p. 425.8 (5) K. The hydrogen-bonding schemes in these structures have been analysed and compared with the hydrogen-bond patterns in the equivalent racemic acids. The structural data from six other structures were included in the analysis, which led to a general description of the great variety of hydrogen-bond motifs observed in α-hydroxycarboxylic acids. Differences between crystal structures of the racemic and enantiomerically pure fluoromandelic acids have been related to their melting enthalpies. The observed differences in the binary phase diagrams of the three acids can be rationalized in terms of their structural differences.

1. Introduction

Interactions between chiral molecules play an important role in the function of drugs, insecticides and herbicides. Using traditional synthetic routes to prepare such compounds will almost invariably lead to a racemate containing both enantiomers. The crystallization of the racemate gives in most cases crystals containing equal amounts of both enantiomers, *i.e.* a racemic compound. The racemic compound formed by the crystallization of a racemate behaves like a pure compound, most frequently it is higher melting than the pure enantiomer. A spontaneous resolution of the racemate may also occur by crystallization, leading to a conglomerate (a mechanical mixture) of crystals each containing one enantiomer.

Assuming an ideal behaviour in the melt, the differences in thermochemical properties and crystallization behaviour of racemates must have their origin in differences in the intermolecular interactions in the crystal. Between molecules of the same chirality they are classified as homo- and heterochiral, if they occur between molecules of opposite chirality.

As part of our investigations into the relations between differences in intermolecular interactions and the different crystallization behaviour of racemates we have studied the monofluoro-substituted mandelic acids. Although the racemates of all three acids crystallize as racemic compounds, only *ortho*-fluoromandelic acid conforms with the most common behaviour that its racemic compound is higher melting than the pure enantiomer. The crystal structures of the three racemic monofluoro-substituted mandelic acids have been reported earlier with their thermodynamic data (Larsen & Marthi, 1994). A preliminary report has been given on the optically active *meta*- and *para*-fluoromandelic acids, but it did not include any structural data (Korver, De Jong & van Soest, 1976). In this paper we present the full structural characterization of the optically active *ortho*-, *meta*- and *para*-fluoromandelic acids, their relation to the structures of the racemic monofluoro-substituted mandelic acids and the thermochemical properties of the racemates and enantiomers.

Since we found a great variation of hydrogen-bond motifs in the fluoromandelic acids, we have investigated if this is a general trend for α-hydroxycarboxylic acids and included results from other structures extracted from the Cambridge Structural Database (Allen *et al.*, 1979) in the analysis.

2. Experimental

The optically active monofluoro-substituted mandelic acids were prepared from the corresponding racemic compounds obtained as reported by Larsen & Marthi (1994). The resolutions were based on the recipes described by Collet & Jacques (1973) and performed similarly for all three compounds. (–)-Ephedrine, (1*R*,2*S*)-(–)-2-(methylamino)-1-phenylpropan-1-ol, was dissolved in ethanol and added to an equimolar amount

† The Centre for Crystallographic Studies is funded by the Danish National Research Foundation.

of the racemic acid dissolved in ethanol. The resulting precipitate was filtered and washed. A recrystallization was performed for the salt of *p*-fluoromandelic acid. The less-soluble diastereomeric salts obtained by these processes were dissolved in a minimum amount of water and eluted through a strong cation ion-exchange column [Lewatit Ionenaustauscher Merck, S1080G1, 0.1–0.2 mm (70–150 mesh ASTM)]. After evaporation of the solvent the acids were purified by recrystallizations from different solvents.

2.1. *o-Fluoromandelic acid*

Racemic *o*-fluoromandelic acid (3.64 g, 21.4 mmol) was resolved with 3.53 g (21.4 mmol) of (–)-ephedrine to give 3.25 g (9.7 mmol, 91% for one enantiomer) of the less-soluble diastereomeric salt.

The isolated acid {1.59 g, 9.3 mmol, $[\alpha]_{578}^{20} = -135.6$ ($c = 1.1$, acetone)} was recrystallized first from benzene, then from chloroform to give the optically pure compound as a white crystalline powder, $[\alpha]_{578}^{20} = -142.7$ ($c = 1.2$, acetone). Crystals suitable for single-crystal diffraction studies were obtained by recrystallization in microtubes from a 2:1 ether:*n*-heptane mixture.

2.2. *m-Fluoromandelic acid*

Racemic *m*-fluoromandelic acid (4.00 g, 23.5 mmol) was resolved with 3.80 g (23.0 mmol) of (–)-ephedrine to give 2.30 g (6.9 mmol, 59%) of the less-soluble diastereomeric salt.

The crude acid obtained by ion exchange was recrystallized from benzene to give 0.90 g (5.3 mmol, 45%) of a white silky crystalline powder, $[\alpha]_{578}^{20} = -112.7$ ($c = 1.8$, acetone). The acid was further purified by recrystallization from benzene to obtain the optically pure acid, $[\alpha]_{578}^{20} = -129.5$ ($c = 1.8$, acetone). Crystals suitable for single-crystal diffraction studies were obtained by recrystallization in microtubes from a chloroform:*n*-heptane mixture.

2.3. *p-Fluoromandelic acid*

Racemic *p*-fluoromandelic acid (1.30 g, 7.6 mmol) was resolved with 1.26 g (7.6 mmol) of (–)-ephedrine to give 1.28 g (3.8 mmol, 100%) of a precipitate, which was recrystallized from 10 ml of ethanol to give 0.71 g (2.1 mmol, 55%) of the less-soluble diastereomeric salt. Recrystallization of the crude acid from ethanol resulted in the optically pure acid as a white crystalline powder, $[\alpha]_{578}^{20} = -144.4$ ($c = 1.0$, acetone). Crystals for the single-crystal diffraction study were obtained from a batch prepared by the method described by Collet & Jacques (1973). The precipitate containing both diastereomeric salts was recrystallized and dissolved in 5 *M* aqueous HCl. The precipitated acid [10 mg, enough material for a differential scanning calorimetry (DSC) measurement] was removed by filtration. The mother liquor was left at room temperature. After evaporation of the liquid, beautiful white crystals suitable for single-crystal X-ray diffraction studies appeared. The DSC analysis of a representative sample showed that it was a mechanical mixture of racemic and enantiomeric crystals. This was confirmed by the examination of the crystals under a microscope; one of the crystals that differed from the earlier studied racemic form was selected for the diffraction study.

2.4. *Thermochemical measurements*

Melting points and heats of fusion were measured by DSC using a PL-DSC instrument calibrated with indium and tin. The measurements were carried out under a nitrogen atmosphere in open crucibles. Sampling was made every 1.25 s and a heating rate of 5 K min^{-1} was used. The mass of each sample was between 3.2 and 3.3 mg. They were measured with a precision of 0.001 mg. The samples of the optically pure compounds showed sharp reproducible melting, proving that the compounds were pure. The associated melting enthalpies were determined with a reproducibility of 5%. Thermogravimetric measurements on optically active *ortho-* and *meta*-fluoromandelic acid samples showed that no weight loss occurred in the investigated temperature range, whereas a weight loss of up to 3% was observed for the optically active *para*-fluoromandelic acid before melting. The DSC curves recorded for the *o-* and *m*-fluoromandelic acids at different stages of the purification process were found to be in agreement with the calculated binary phase diagram.

2.5. *Spectroscopic measurements*

Optical rotations were measured at room temperature at 578 nm (Hg) with a Perkin–Elmer 241 polarimeter and were used to calculate the optical purity of the compounds. Literature values (Collet & Jacques, 1973) are: *o*-fluoromandelic acid: $[\alpha]_{578} = 145$ (acetone, $c = 1.2$), *m*-fluoromandelic acid: $[\alpha]_{578} = 129$ (acetone, $c = 1.8$), *p*-fluoromandelic acid: $[\alpha]_{578} = 140$ (acetone, $c = 1$). The ^{13}C NMR spectra were recorded at 298 K using a Varian Unity 400 spectrometer. The measurements were performed on 10 mg of sample dissolved in 500 µl of dimethyl sulfoxide. The spectra show the same characteristics as the spectra of the corresponding racemic compounds. The signals of the C atoms in the phenyl rings appear as doublets due to coupling with fluorine. The ^{13}C NMR spectra of all three compounds can be assigned using the chemical shifts and the coupling constants of CH_2OH and F substituents. The labelling of the atoms refers to Fig. 1. An unambiguous assignment could not be made for the signals arising from C6 and C8 in *o*-fluoromandelic acid and from C4 and C6 in the *m*-fluoromandelic acid. Measured chemical shifts in p.p.m. relative to TMS: *o*-Fluoromandelic acid: 66.44 (d, $J = 2.3$ Hz, C2); 115.28 (d, $J = 21.3$ Hz, C5); 124.40 (d, $J = 3.0$ Hz, C7); 127.65 (d, $J = 14.5$ Hz, C3); 128.88 (d, $J = 4.5$ Hz) and 129.80 (d, $J = 7.5$ Hz, C6 and C8); 159.63 (d, $J = 245.7$ Hz, C4); 173.312 (C1).

m-Fluoromandelic acid: 71.788 (C2); 113.25 (d, J = 22.1 Hz) and 114.41 (d, J = 20.6 Hz, C4 and C6); 122.67 (d, J = 3.1 Hz, C8); 130.11 (d, J = 7.6 Hz, C7); 143.09 (d, J = 6.8 Hz, C3); 162.02 (d, J = 242.7 Hz, C5); 173.570 (C1). *p*-Fluoromandelic acid: 72.014 (C2); 115.24 (d, J = 21.4 Hz, C5 and C7); 128.94 (d, J = 8.4 Hz, C4 and C8); 136.830 (C3); 161.97 (d, J = 243.4 Hz, C6); 174.267 (C1).

2.6. *Structure determinations*

Optically active *para*-fluoromandelic acid was characterized by room-temperature Weissenberg photographs and its space group assigned from the systematically absent reflections.

CAD-4 diffractometers equipped with graphite monochromators were used for the data collections. The quality of the crystals was decisive for our choice of wavelength used for the diffraction experiment. Only the crystals of optically active *para*-fluoromandelic acid were so well diffracting that it enabled us to use Mo $K\alpha$ (λ = 0.71073 Å) radiation for the data collection. Cu $K\alpha$ (λ = 1.54184 Å) radiation was used for optically active *ortho*- and *meta*-fluoromandelic acids. The crystals were cooled with Enraf–Nonius gas-flow

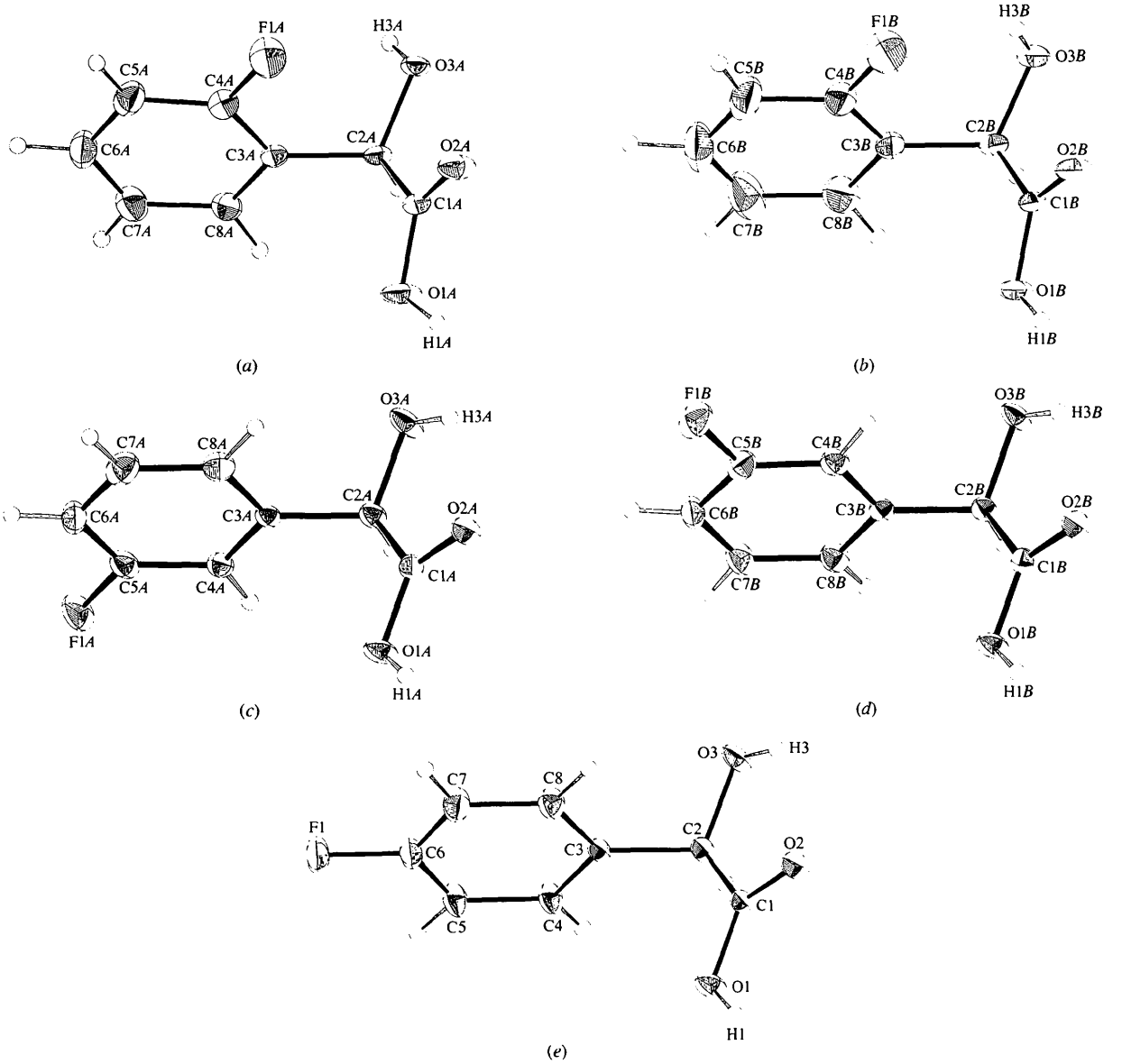

Fig. 1. *ORTEP*II (Johnson, 1976) drawings showing the molecular geometry of the monofluoro-substituted mandelic acids in the crystals of the pure enantiomers. The thermal ellipsoids are scaled to include 50% probability. The H atoms are drawn as spheres with a fixed radius. (*a*) and (*b*) *ortho*-, (*c*) and (*d*) *meta*-, and (*e*) *para*-fluoromandelic acid.

Table 1. *Experimental details*

	OO	OM	OP
Crystal data			
Chemical formula	$FC_6H_4CH(OH)COOH$	$FC_6H_4CH(OH)COOH$	$FC_6H_4CH(OH)COOH$
Chemical formula weight	170.14	170.14	170.14
Cell setting	Monoclinic	Monoclinic	Monoclinic
Space group	$P2_1$	$P2_1$	$C2$
a (Å)	8.356 (2)	8.493 (3)	8.464 (2)
b (Å)	10.842 (2)	5.8426 (7)	5.8518 (13)
c (Å)	8.544 (2)	15.628 (3)	15.868 (2)
β (°)	94.13 (2)	104.10 (2)	107.56 (2)
V (Å^3)	772.0 (3)	752.1 (3)	749.3 (3)
Z	4	4	4
D_x (Mg m^{-3})	1.464	1.503	1.508
Radiation type	Cu $K\alpha$	Cu $K\alpha$	Mo $K\alpha$
Wavelength (Å)	1.54184	1.54184	0.71073
No. of reflections for cell parameters	20	20	22
θ range (°)	40.27–46.31	37.76–45.55	19.44–21.32
μ (mm^{-1})	1.067	1.096	0.131
Temperature (K)	122.0 (5)	112.0 (5)	122.0 (5)
Crystal form	Needle	Needle	Cubic
Crystal size (mm)	0.48 × 0.15 × 0.08	0.40 × 0.12 × 0.04	0.25 × 0.25 × 0.25
Crystal colour	White	White, silky	White
Data collection			
Diffractometer	Enraf–Nonius CAD-4	Enraf–Nonius CAD-4	Enraf–Nonius CAD-4
Data collection method	ω–2θ scans	ω–2θ scans	ω–2θ scans
Absorption correction	Integration	Integration	None
T_{min}	0.719	0.770	–
T_{max}	0.919	0.956	–
No. of measured reflections	5818	5815	3552
No. of independent reflections	3181	3096	3307
No. of observed reflections	3119	2810	2977
Criterion for observed reflections	$I > 2\sigma(I)$	$I > 2\sigma(I)$	$I > 2\sigma(I)$
R_{int}	0.0182	0.0192	0.0160
θ_{max} (°)	74.83	74.88	45.29
Range of h, k, l	$-10 \rightarrow h \rightarrow 6$ $-13 \rightarrow k \rightarrow 13$ $-10 \rightarrow l \rightarrow 10$	$-10 \rightarrow h \rightarrow 10$ $-7 \rightarrow k \rightarrow 7$ $-19 \rightarrow l \rightarrow 19$	$0 \rightarrow h \rightarrow 16$ $0 \rightarrow k \rightarrow 11$ $-31 \rightarrow l \rightarrow 30$
No. of standard reflections	5	5	3
Frequency of standard reflections (min)	166.7	166.7	166.7
Intensity decay (%)	4.5	11.5	0.2
Refinement			
Refinement on	F^2	F^2	F^2
$R[F^2 > 2\sigma(F^2)]$	0.0287	0.0292	0.0356
$wR(F^2)$	0.0759	0.0873	0.1134
S	1.104	1.052	1.121
No. of reflections used in refinement	3181	3095	3301
No. of parameters used	259	260	130
H-atom treatment	Only coordinates of H atoms refined	Only coordinates of H atoms refined	Only coordinates of H atoms refined
Weighting scheme	$w = 1/[\sigma^2(F_o^2) + (0.0505P)^2 + 0.0714P]$, where $P = (F_o^2 + 2F_c^2)/3$	$w = 1/[\sigma^2(F_o^2) + (0.0559P)^2 + 0.0267P]$, where $P = (F_o^2 + 2F_c^2)/3$	$w = 1/[\sigma^2(F_o^2) + (0.0497P)^2 + 0.1016P]$, where $P = (F_o^2 + 2F_c^2)/3$
$(\Delta/\sigma)_{max}$	0.001	0.002	0.001
$\Delta\rho_{max}$ (e Å^{-3})	0.261	0.206	0.385
$\Delta\rho_{min}$ (e Å^{-3})	−0.221	−0.216	−0.309
Extinction method	None	*SHELXL*93 (Sheldrick, 1993)	None
Extinction coefficient	–	0.0104 (9)	–
Source of atomic scattering factors	*International Tables for Crystallography* (1992, Vol. C, Tables 4.2.6.8 and 6.1.1.4)	*International Tables for Crystallography* (1992, Vol. C, Tables 4.2.6.8 and 6.1.1.4)	*International Tables for Crystallography* (1992, Vol. C, Tables 4.2.6.8 and 6.1.1.4)
Absolute configuration	−0.05 (10) (Flack, 1983)	−0.04 (11) (Flack, 1983)	–

low-temperature devices. The temperatures, 122 (for *ortho-* and *para-*) and 112 K (for *meta*-fluoromandelic acid), were monitored with a thermocouple placed a few centimetres above the crystal in the exhaust pipe. They remained constant within 1 K during the three data collections. In each case an analysis of reflection profiles provided the basis for the selection of scan mode and scan interval. The different experimental conditions with information on the data reduction and refinement results are summarized in Table 1. The intensities of standard reflections were measured after every 10 000 s. The orientation of each crystal was checked after every

300 reflections. The reflections used for the intensity control showed a systematic decay for *ortho-* and *meta*-fluoromandelic acid. Corrections were made for these variations, using a polynomial fit up to third order. The data reduction, performed with the *DREADD* data reduction package (Blessing, 1987), also included corrections for Lorentz, polarization, background and absorption; the latter effect was taken into consideration only for the data sets collected with Cu $K\alpha$ radiation (*ortho-* and *meta*-fluoromandelic acids). Averaging was performed for the reflections related by the symmetry of the crystal class.

The structure for optically active *ortho-* and *para*-fluoromandelic acid were solved by direct methods, *SHELXS*86 (Sheldrick, 1990). Although the systematically absent reflections show that optically active *meta*-fluoromandelic acid crystallizes in space group $P2_1$, all hkl reflections with $h + k = 2n + 1$ were systematically weak. Attempts to solve the crystal structure in $P2_1$ with the default settings in *SHELXS*86 (Sheldrick, 1990) were fruitless. The determination of the crystal structure was finally achieved by two different methods. We had noted that the optically active mandelic acid crystallizes in $P2_1$ with cell dimensions very similar to those of *meta*-fluoromandelic acid. The known coordinates of the C and O atoms of (*S*)-(+)-mandelic acid (Patil, Pennington, Paul, Curtin & Dykstra, 1987) were used to calculate the difference-electron-density map which showed the position of the F atoms. The structure could also be solved by direct methods if the space group was assumed to be *C*2, thereby omitting all the weak reflections ($h + k = 2n + 1$). This gave a solution corresponding to the average structure of the non-centred cell.

The three structures were refined by full-matrix least-squares with *SHELXL*93 (Sheldrick, 1993), minimizing $\Sigma w(F_o^2 - F_o^2)^2$. The scattering factors were taken from *International Tables for Crystallography* (1992, Vol. C) and used as contained in the program. After anisotropic displacement parameters had been introduced for the non-H atoms, the calculated difference-Fourier maps showed the positions for all the H atoms. Their positional parameters were included in the refinements and given isotropic displacement parameters equal to U_{eq} of the parent C or O atom multiplied by 1.2 and 1.5, respectively. Polar axis restraints were applied according to the method of Flack & Schwarzenbach (1988). For optically active *ortho-* and *meta*-fluoromandelic acids the absolute configuration was established by refinement of the absolute structure parameter, x (Flack, 1983). As expected, the value of x in the crystal structure of optically active *para*-fluoromandelic acid, measured with Mo $K\alpha$ radiation, could not be estimated reliably. The absolute configuration of the acid was set to the known absolute configuration for the acid obtained from the precipitating salt (Korver, 1970).

An extinction correction was employed to the data of *meta*-fluoromandelic acid. The final fractional coordinates for all three structures are listed in Table 2.* The only features in the final residual electron-density maps could be associated with bonding electrons and the lone pairs of the O and F atoms.

3. Results and discussion

In this paragraph we give a description of the molecular structures of the optically active monofluoro-substituted mandelic acids followed by a comparison with the corresponding molecules in the racemic compounds. This leads to a systematic survey of the possible hydrogen-bond modes of α-hydroxycarboxylic acids. Finally, a description will be given of the relations between the crystal structures of the racemic and enantiomeric monofluoro-substituted mandelic acids and their thermochemical properties. Throughout this section we will refer to the compounds by a two-letter combination. The first letter **O** indicates optically active and **R** racemic; the second letter can be **O**, **M** and **P** for *ortho-*, *meta-* and *para*-fluoromandelic acid, respectively.

3.1. *Molecular structures*

The NMR spectra of the racemic and enantiomeric monofluoro-substituted mandelic acids did not show any differences, therefore, the observed variations in the conformation of the acids must be due to differences in the crystal packing.

The two molecules in the asymmetric unit of the crystal structures of *ortho-* and *meta*-substituted acids (**OO** and **OM**) are distinguished by letters *A* and *B*. The molecular geometry of the five different monofluoro-substituted mandelic acids are illustrated by the drawings in Fig. 1 and by Table 3. C4 is chosen to make F attached to the smallest possible number in the phenyl ring. The bond lengths and angles are virtually identical to those found in the racemic acids. The bond angles in the phenyl ring show the same deviations from the idealized 120° as described for the racemic compounds due to the F and CH(OH)COOH substitutions (Larsen & Marthi, 1994).

The conformation of the *para*-substituted mandelic acid is, similar to the unsubstituted mandelic acid, uniquely determined by the two torsion angles O2—C1—C2—O3 and C1—C2—C3—C4, but for the *ortho-* and *meta*-substituted acids an additional parameter is necessary, which defines the position of fluorine relative to the hydroxy group.

The conformation of the two independent molecules in **OO** is almost identical. Although the orientation of the phenyl groups is very similar to the orientation found

* Lists of atomic coordinates, anisotropic displacement parameters and structure factors have been deposited with the IUCr (Reference: AB0363). Copies may be obtained through The Managing Editor, International Union of Crystallography, 5 Abbey Square, Chester CH1 2HU, England.

Table 2. *Fractional atomic coordinates and equivalent isotropic displacement parameters (Å²)*

$U_{eq} = (1/3)\Sigma_i\Sigma_j U^{ij} a_i^* a_j^* \mathbf{a}_i.\mathbf{a}_j.$

	x	y	z	U_{eq}
(*R*)-(−)-*ortho*-Fluoromandelic acid (**OO**)				
F1*A*	0.34049 (13)	0.66467 (8)	1.18255 (11)	0.0328 (2)
O1*A*	0.75581 (11)	0.50971 (11)	1.07102 (13)	0.0262 (2)
H1*A*	0.833 (3)	0.560 (2)	1.017 (3)	0.039
O2*A*	0.58359 (12)	0.62106 (10)	0.91438 (13)	0.0245 (2)
O3*A*	0.34445 (11)	0.46666 (9)	0.96276 (11)	0.0166 (2)
H3*A*	0.281 (2)	0.415 (2)	1.003 (2)	0.025
C1*A*	0.61158 (15)	0.53759 (13)	1.0059 (2)	0.0160 (2)
C2*A*	0.48632 (15)	0.44990 (12)	1.06291 (15)	0.0149 (2)
C3*A*	0.45971 (15)	0.47030 (13)	1.23465 (15)	0.0162 (2)
C4*A*	0.3820 (2)	0.57384 (13)	1.2867 (2)	0.0215 (3)
C5*A*	0.3455 (2)	0.58900 (15)	1.4409 (2)	0.0269 (3)
C6*A*	0.3951 (2)	0.4999 (2)	1.5493 (2)	0.0296 (3)
C7*A*	0.4767 (2)	0.3966 (2)	1.5027 (2)	0.0287 (3)
C8*A*	0.5079 (2)	0.38147 (13)	1.3461 (2)	0.0215 (3)
F1*B*	−0.22623 (13)	0.61539 (12)	0.64763 (13)	0.0418 (3)
O1*B*	0.22070 (11)	0.67465 (10)	0.84435 (12)	0.0214 (2)
H1*B*	0.272 (3)	0.610 (2)	0.886 (3)	0.032
O2*B*	0.01542 (11)	0.58842 (9)	0.95690 (13)	0.0230 (2)
O3*B*	−0.16988 (11)	0.79302 (10)	0.89393 (12)	0.0193 (2)
H3*B*	−0.226 (3)	0.736 (2)	0.869 (3)	0.029
C1*B*	0.07107 (15)	0.67121 (13)	0.88111 (14)	0.0162 (2)
C2*B*	−0.02499 (14)	0.78253 (13)	0.81850 (15)	0.0166 (3)
C3*B*	−0.0462 (2)	0.78004 (13)	0.6408 (2)	0.0201 (3)
C4*B*	−0.1466 (2)	0.6960 (2)	0.5621 (2)	0.0276 (3)
C5*B*	−0.1689 (2)	0.6905 (2)	0.4001 (2)	0.0400 (4)
C6*B*	−0.0857 (3)	0.7717 (2)	0.3132 (2)	0.0455 (5)
C7*B*	0.0179 (3)	0.8571 (2)	0.3874 (2)	0.0460 (5)
C8*B*	0.0369 (2)	0.8614 (2)	0.5502 (2)	0.0327 (4)
(*R*)-(−)-*meta*-Fluoromandelic acid (**OM**)				
F1*A*	0.18461 (10)	0.5963 (3)	0.91553 (5)	0.0289 (2)
O1*A*	0.31847 (13)	0.1574 (2)	0.63407 (7)	0.0208 (2)
H1*A*	0.350 (2)	0.041 (5)	0.6130 (14)	0.031
O2*A*	0.45835 (12)	0.3254 (2)	0.54619 (6)	0.0190 (2)
O3*A*	0.39150 (14)	0.7445 (2)	0.59253 (7)	0.0239 (3)
H3*A*	0.436 (2)	0.689 (4)	0.5521 (14)	0.036
C1*A*	0.3750 (2)	0.3341 (3)	0.59933 (8)	0.0138 (3)
C2*A*	0.32239 (15)	0.5625 (2)	0.63116 (8)	0.0151 (3)
C3*A*	0.37105 (14)	0.5795 (3)	0.73088 (7)	0.0142 (2)
C4*A*	0.25209 (14)	0.5809 (3)	0.77847 (8)	0.0164 (2)
C5*A*	0.3011 (2)	0.5942 (3)	0.86947 (8)	0.0198 (3)
C6*A*	0.4620 (2)	0.6065 (3)	0.91529 (8)	0.0233 (3)
C7*A*	0.5788 (2)	0.6053 (4)	0.86700 (9)	0.0248 (3)
C8*A*	0.53509 (14)	0.5937 (4)	0.77537 (8)	0.0203 (3)
F1*B*	−0.24318 (9)	0.5986 (3)	0.08989 (5)	0.0289 (2)
O1*B*	0.18017 (13)	0.1648 (2)	0.36567 (7)	0.0204 (2)
H1*B*	0.147 (2)	0.037 (4)	0.3869 (14)	0.031
O2*B*	0.04074 (12)	0.3322 (2)	0.45368 (6)	0.0191 (2)
O3*B*	0.09927 (14)	0.7521 (2)	0.40344 (7)	0.0210 (2)
H3*B*	0.064 (2)	0.703 (4)	0.4444 (14)	0.032
C1*B*	0.1223 (2)	0.3411 (3)	0.39988 (8)	0.0133 (3)
C2*B*	0.17127 (14)	0.5697 (3)	0.36623 (8)	0.0145 (3)
C3*B*	0.12198 (14)	0.5828 (3)	0.26652 (7)	0.0143 (2)
C4*B*	−0.04337 (14)	0.5867 (3)	0.22315 (8)	0.0175 (2)
C5*B*	−0.08349 (15)	0.5964 (3)	0.13220 (8)	0.0203 (3)
C6*B*	0.0299 (2)	0.6027 (3)	0.08234 (8)	0.0229 (3)
C7*B*	0.1929 (2)	0.6001 (4)	0.12628 (8)	0.0237 (3)
C8*B*	0.23900 (14)	0.5899 (3)	0.21839 (8)	0.0191 (3)
(*R*)-(−)-*para*-Fluoromandelic acid (**OP**)				
F	0.25325 (12)	0.22906 (14)	−0.00442 (4)	0.02841 (14)
O1	0.43378 (8)	0.67669 (11)	0.36506 (5)	0.01932 (12)
H1	0.479 (2)	0.802 (4)	0.3854 (12)	0.029
O2	0.66203 (7)	0.50842 (11)	0.45392 (4)	0.01756 (10)
O3	0.54978 (9)	0.09045 (11)	0.40495 (5)	0.02094 (13)
H3	0.629 (2)	0.128 (5)	0.4438 (13)	0.031
C1	0.52524 (8)	0.49977 (12)	0.39993 (4)	0.01222 (9)
C2	0.44132 (9)	0.27279 (12)	0.36670 (4)	0.01308 (10)
C3	0.39024 (8)	0.25790 (12)	0.26699 (4)	0.01264 (9)
C4	0.22379 (9)	0.2540 (2)	0.21803 (5)	0.01890 (13)
C5	0.17592 (11)	0.2436 (2)	0.12596 (5)	0.0230 (2)
C6	0.29861 (12)	0.2381 (2)	0.08526 (5)	0.01957 (13)
C7	0.46518 (12)	0.2404 (2)	0.13146 (6)	0.0229 (2)
C8	0.51075 (10)	0.2496 (2)	0.22336 (5)	0.01953 (13)

in the racemic crystal they differ with respect to the position of the F atom. In **OO** the two molecules show F substitution adjacent to the hydroxy group; in **RO** it is on the opposite side. The two independent molecules in **OM** have very similar phenyl-group orientations, but they differ with respect to F substitution. In molecule *A* it is found on the opposite side relative to molecule *B*, which adopts a conformation similar to the conformation of the two independent molecules in its racemic counterpart, **RM**. In **RM** the conformation of the phenyl group in the two molecules differs by *ca* 15°. The two molecules in **OM** are almost related by a translational symmetry of **a**/2 + **b**/2; the only atom which does not approximately obey this pseudo-symmetry is F. Had the F substitution occurred on the same side of both molecules the crystal structure would have space-group symmetry *C*2. This could explain the earlier assignment of the space group to be *C*2 (Cesario, Guilhem, Pascard, Collet & Jacques, 1978) based on the results from the paper by Korver, De Jong & van Soest (1976).

OP crystallizes in space group *C*2 with one molecule in the asymmetric unit with an orientation of the phenyl group that differs slightly (~15°) from the orientation found in **RP**.

The α-hydroxy substitution appears to have a significant effect on the conformation of the C3—C2—C1—O2 moiety. In his analysis of the packing modes for carboxylic acids Leiserowitz (1976) found that the fragment CR_2—CR_2—C=O in saturated carboxylic acids is synplanar with a torsion angle around 0°. In the α-hydroxy acids it is rather the O3—C2—C1=O2 torsion angle which is close to 0°. An intramolecular O3—H3···O2 hydrogen bond is often observed in the α-hydroxy acids which restrains the O3—C2—C1—O2 torsion angle to values close to 0°. This intramolecular hydrogen bond is not a requirement for a small torsion angle, as exemplified by **RO**, which does not form an intramolecular hydrogen bond but still has the lowest O3—C2—C1—O2 torsion angle of 2.3 (2)°, and **RP**, which has an intramolecular hydrogen bond and rather a large O3—C2—C1—O2 torsion angle of −12.11 (14)°.

The optically active fluoromandelic acids have their phenyl groups in virtually the same orientation in the crystals, the C1—C2—C3—C4(C8) torsion angles only differ by *ca* 5°. These torsion angles display a much larger variation (36°) in the racemic compounds. With the exception of molecule *B* in **OM** the C1—C2—C3—C4 torsion angle has the same sign as the O2—C1—C2—O3 torsion angle [for the

Table 3. *Bond distances (Å), and bond and selected torsion angles (°) in the optically active monofluoro-substituted mandelic acids*

	OO molecule *A*	**OO** molecule *B*	**OM** molecule *A*	**OM** molecule *B*	**OP**
F1—C(4,5,6)	1.355 (2)	1.346 (2)	1.3580 (14)	1.3564 (14)	1.3585 (10)
O1—C1	1.326 (2)	1.311 (2)	1.310 (2)	1.310 (2)	1.3111 (10)
O2—C1	1.208 (2)	1.218 (2)	1.217 (2)	1.214 (2)	1.2159 (9)
O3—C2	1.423 (2)	1.416 (2)	1.419 (2)	1.422 (2)	1.4190 (10)
C1—C2	1.520 (2)	1.525 (2)	1.528 (2)	1.530 (2)	1.5234 (10)
C2—C3	1.516 (2)	1.516 (2)	1.515 (2)	1.514 (2)	1.5116 (10)
C3—C4	1.386 (2)	1.380 (2)	1.393 (2)	1.403 (2)	1.3887 (10)
C3—C8	1.393 (2)	1.391 (2)	1.400 (2)	1.385 (2)	1.3958 (11)
C4—C5	1.384 (2)	1.385 (2)	1.383 (2)	1.380 (2)	1.3946 (11)
C5—C6	1.381 (2)	1.373 (3)	1.381 (2)	1.379 (2)	1.3789 (14)
C6—C7	1.384 (3)	1.389 (4)	1.385 (2)	1.387 (2)	1.3789 (13)
C7—C8	1.391 (2)	1.390 (3)	1.391 (2)	1.398 (2)	1.3924 (12)
O2—C1—O1	124.79 (12)	123.72 (12)	125.62 (13)	125.65 (13)	125.45 (7)
O2—C1—C2	124.79 (12)	123.92 (12)	121.57 (12)	121.64 (13)	121.71 (7)
O1—C1—C2	110.42 (11)	112.36 (11)	122.80 (11)	112.70 (11)	112.84 (6)
O3—C2—C3	112.92 (10)	114.52 (11)	110.57 (11)	110.15 (11)	110.37 (6)
O3—C2—C1	106.88 (10)	110.46 (11)	109.39 (11)	109.50 (11)	109.49 (6)
C3—C2—C1	111.81 (11)	110.96 (11)	111.34 (11)	111.59 (11)	111.64 (6)
C4—C3—C8	117.36 (12)	117.25 (14)	119.87 (11)	120.21 (11)	119.45 (7)
C4—C3—C2	122.23 (12)	121.50 (13)	119.87 (11)	119.43 (11)	120.54 (7)
C8—C3—C2	120.36 (12)	121.24 (14)	120.26 (11)	120.35 (11)	120.01 (6)
F1—C(4,5,6)—C(5,6,7)	118.37 (13)	118.6 (2)	118.77 (11)	118.52 (11)	118.54 (9)
F1—C(4,5,6)—C(3,4,5)	118.79 (12)	118.13 (13)	118.01 (11)	117.98 (11)	118.47 (8)
C5—C4—C3	122.84 (14)	123.3 (2)	118.26 (11)	117.73 (11)	120.79 (8)
C6—C5—C4	118.61 (14)	118.4 (2)	123.22 (11)	123.50 (11)	118.02 (7)
C5—C6—C7	120.27 (14)	120.3 (2)	117.82 (12)	118.04 (11)	122.99 (7)
C6—C7—C8	120.1 (2)	120.1 (2)	120.94 (12)	120.36 (11)	118.22 (8)
C7—C8—C3	120.76 (14)	120.7 (2)	119.88 (11)	120.16 (11)	120.52 (7)
O2—C1—C2—O3	13.3 (2)	15.5 (2)	−2.6 (2)	−3.4 (2)	−2.77 (9)
C1—C2—C3—C4	71.2 (2)	71.5 (2)	−112.2 (2)	66.4 (2)	−112.69 (9)

racemic *para*-fluoro compound the numbering scheme reported by Larsen & Marthi (1994) for C4 and C8 should be reversed]. We have noticed an apparent relation between the torsion angles O2—C1—C2—O3 and C1—C2—C3—C4(C8). If the first torsion angle is larger than 12°, the numerical value of the torsion angle C1—C2—C3—C4 is smaller than that of C1—C2—C3—C8. The relative magnitude of C1—C2—C3—C4 and C1—C2—C3—C8 is reversed if the torsion angle O2—C1—C1—O3 is close to 0° (*i.e.* 2–3°). Molecule *B* in **OM** is the only molecule which does not conform to this pattern. Analysis of the crystal packing has revealed the reason. Very similar hydrogen-bonding schemes are observed in **OM** and **OP** (*vide infra*), apart from the position of the F substitution, the two structures are almost isostructural. The deviation from *C*2 symmetry in **OM** is due to the different substitution of F, which prevents unfavourable intermolecular F···F contacts. If the F atom on molecule *B* was introduced as in molecule *A* it would lead to a F···F distance of *ca* 2.6 Å.

The positions of the two H atoms H1 and H3 are useful to have in mind for the analysis of the hydrogen bonding (Table 2). The H atom of the carboxylic acid group in these systems is as expected in the *syn* configuration (Leiserowitz, 1976), whereas the H atom of the hydroxy group is free to rotate around the C3—O3 bond. Its position appears to be affected by two competing interactions: with F and O2, leading to the formation of a hydrogen bond. The molecular drawings in Fig. 1 show that the electrostatic interaction with F seems to influence the stereochemistry in **OO**. In **RO** this interaction is not observed, since F is found on the opposite side of the molecule relative to **OO**.

3.2. *Crystal packing*

Our discussion of the crystal packing focuses mainly on the O—H···O hydrogen bonds, since they represent the strongest intermolecular interactions in the crystal packings shown in Figs. 2–4. The C1···F electrostatic interactions observed for racemic *ortho*- and *para*-fluoromandelic acids are not observed in the structures of the optically active compounds.

3.3. *O—H···O hydrogen bonds in α-hydroxycarboxylic acids*

A general description of all the possible hydrogen bonds in α-hydroxycarboxylic acids will be followed by an analysis of the crystal packing in the optically active fluoromandelic acids. A search was made in the

Cambridge Structural Database, Version 5.09 (Allen *et al.*, 1979), to extract structural data for all α-hydroxycarboxylic acids without other functional groups capable of hydrogen bonding. This enabled us to include six additional structures in the analysis besides the six racemic and optically active fluoromandelic acids. Analysis of the crystal structures were performed with *Cerius*[2] (Biosym Technologies, 1995) and *PLATON* (Spek, 1990). In the subsequent discussion the labelling will refer to that used for fluoromandelic acids. α-Hydroxycarboxylic acids contain two donor groups, O3—H3 and O1—H1, and three potential acceptor atoms (O1, O2 and O3) if one only considers O—H···O hydrogen bonds. The intramolecular O1—H1···O2 hydrogen bond is sterically hindered and of the other possible intramolecular hydrogen bonds (O1—H1···O3, O3—H3···O1 and O3—H3···O2) only the O3—H3···O2 hydrogen bond is observed. In all the investigated structures the common structural fragment adopts a conformation where the O2—C1—C2—O3 torsion angle is small, which excludes the formation of intramolecular O3—H3···O1 and O1—H1···O3 hydrogen bonds.

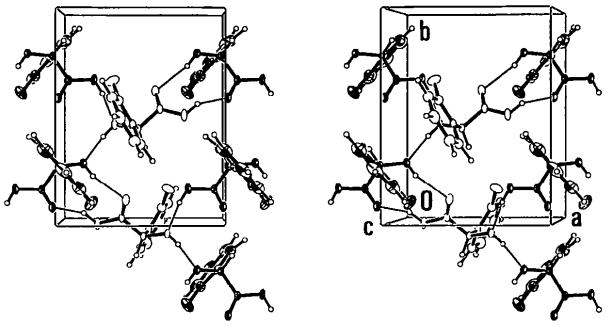

Fig. 2. Stereo pair (Johnson, 1976) illustrating the packing in *ortho*-fluoromandelic acid as seen along the **c** axis. The O—H···O hydrogen bonds are shown as thin lines. Molecules labelled *B* are drawn as shaded ellipsoids.

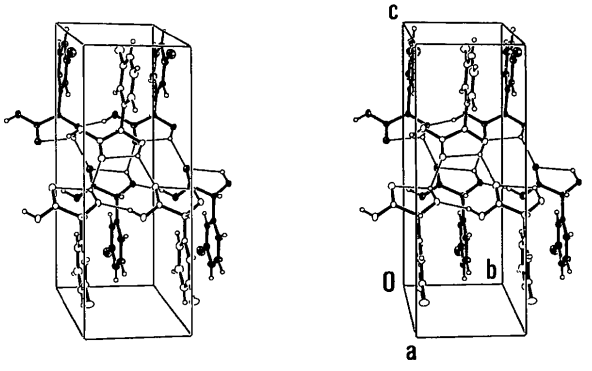

Fig. 3. Stereo pair (Johnson, 1976) illustrating the packing in *meta*-fluoromandelic acid as seen along the **a** axis. The O—H···O hydrogen bonds are shown as thin lines. Molecules labelled *B* are drawn as shaded ellipsoids.

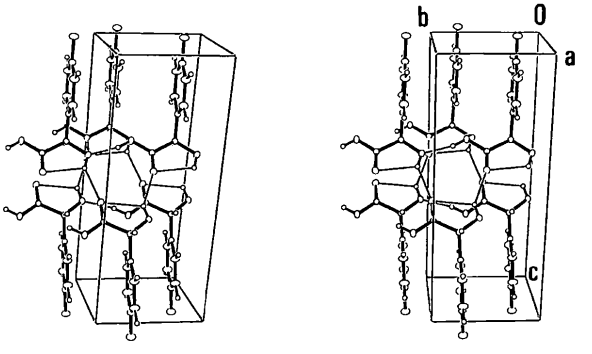

Fig. 4. Stereo pair (Johnson, 1976) illustrating the packing in *para*-fluoromandelic acid as seen along the **a** axis. The O—H···O hydrogen bonds are shown as thin lines.

An overview of the possible intermolecular O—H···O hydrogen bonds is given in Table 4. They are grouped according to their first-level graph-set motif (Bernstein, Davis, Shimoni & Chang, 1995). It is also indicated whether the hydrogen bonds link molecules of the same or opposite chirality. The limited structural information available made it reasonable to consider only the symmetry elements we encountered in the structures, *i.e.* translation, twofold axis, twofold screw axis, glide plane and inversion. Four of the six structures extracted from CSD are racemates (refcodes DLHTDA10, DLMAND01, GLICAC10 and HXIBAC) and two crystallize in chiral space groups (FEGHAA and PLACTA). It is noteworthy that two of the structures (GLICAC10 and HXIBAC) which do not contain any chiral centres adopt a chiral conformation in the crystal. The structures of racemic mandelic acid (DLMAND01) and its enantiomer (FEGHAA) are also part of this analysis. They are found to be isostructural with the corresponding *para*- and *meta*-fluoromandelic acids. Five crystal structures contain two molecules in the asymmetric unit. In two of these (FEGHAA and **OM**) separate hydrogen-bonding patterns are formed by each type of molecule. Hydrogen bonds between two independent molecules in the asymmetric unit (graph set notation D) are shown separately in Table 4.

In **OO** and **RM** the hydrogen bonds are exclusively formed between crystallographically different molecules, whereas the GLICAC10 contains hydrogen bonds between the same type and the two different types of molecules. It is obvious from Table 4 that the α-hydroxycarboxylic acids display a large variety of hydrogen bonds. This is in striking contrast to the β-hydroxycarboxylic acids (Larsen & Marthi, 1995), which contain the same hydrogen-bonding arrangement of identical donor and acceptor atoms. The difference in hydrogen-bond patterns between α- and β-hydroxycarboxylic acids is even more pronounced, if one considers a combination of the two- and three-centre and intramolecular hydrogen bonds.

Table 4. *Hydrogen-bonding patterns in α-hydroxycarboxylic acids*

		Same chirality		Opposite chirality	
D—H···*A*	N_1	Symmetry	Example	Symmetry	Example
O1—H1···O1		-		-	
O1—H1···O2		-	**OO** *A*→*B*	-	RM *A*→*B*
O1—H1···O3	*D*	-	**OO** *B*→*A*	-	RM *A*→*B* RM *B*→*A*
O3—H3···O1		-		-	
O3—H3···O2		-	GLICAC10 *A*→*B* **OO** *B*→*A*	-	GLICAC10 *B*→*A* RM *A*→*B*
O3—H3···O3		-	**OO** *A*→*B*	-	RM *A*→*B*
O1—H1···O1	*C*(2)	2_1 or translation		Glide plane	
O1—H1···O2	$R_2^2(8)$	2		$\bar{1}$	DLHTDA10 RO
	C(4)	2_1 or translation		Glide plane	
O1—H1···O3	*C*(5)	2_1 or translation	PLACTA DLMAND01 GLICAC10 molecule *A* GLICAC10 molecule *B* FEGHAA mol *A* FEGHAA mol *B* HXIBAC RP **OP** **OM** molecule *A* **OM** molecule *B*	Glide plane	
O3—H3···O1	*C*(5)	2_1 or translation	DLHTDA10	Glide plane	
O3—H3···O2	$R_2^2(10)$	2		$\bar{1}$	DLMAND01 HXIBAC RP
	C(5)	2_1 or translation	PLACTA FEGHAA **OP** **OM** molecule *A* **OM** molecule *B*	Glide plane	
O3—H3···O3	*C*(2)	2_1 or translation	RO	Glide plane	

Structures written with open letters contain symmetry elements of the second kind. The molecules in GLICAC10 and HXIBAC adopt a chiral conformation, although neither of the molecules contains an asymmetric carbon.

Virtually all types of hydrogen bonds observed in the structures of α-hydroxycarboxylic acids are also found in the crystal structures of the racemic and optically pure monofluoro-substituted mandelic acids. The only type of hydrogen bond which is not found in these systems is the unique O3—H3···O1 hydrogen bond observed in DLHTDA10. This is the only case where O1 acts as an acceptor for a hydrogen bond. In this system the presence of a 12 C-atom long alkyl chain seems to be a steric hindrance for the formation of other hydrogen bonds. This does not upset the general impression that O1 is a poor acceptor for hydrogen bonds. The carboxylic acid group acts most frequently as a donor to the O atom (O3) of the hydroxy group. Only in a few of the investigated systems (DLHTDA10 and **RO**) is it hydrogen bonded to O2. It should be noted that these interactions lead to the formation of cyclic carboxylic acid dimers and not to the catemers occasionally observed in the crystal packing of carboxylic acids (Bernstein, Etter & Leiserowitz, 1994). The hydroxy groups in these compounds are either hydrogen bonded to themselves (**RO**) or to the carboxylic acid group (DLHTDA10). A schematical drawing of the hydrogen bonds in **RO** is shown in Fig. 5.

Judged from its abundancy the most favourable hydrogen-bond acceptor for the O1—H1 group is the hydroxy group from a molecule related by the symmetry of a twofold screw axis or translation. We notice that these systems also contain intermolecular O3—H3···O2 hydrogen bonds, which connect molecules related by translational symmetry or a twofold screw axis in

PLACTA, FEGHAA, **OP** and **OM**, and molecules related by inversion in **RP**, DLMAND01 and HXIBAC. These motifs are also illustrated in Fig. 5.

With this variety of hydrogen bonds one may wonder which arrangement is the most stable. One of the rules set up for the formation of hydrogen bonds states that the best proton donors establish hydrogen bonds to the best acceptors (Etter, 1991). Knowing that hydrogen bonds are electrostatic interactions one could expect that the charge of the acceptor atom plays an important role. Calculations of charges were performed for the O atoms of the monofluoro-substituted mandelic acids in their crystal geometry (*MOPAC*; *Insight*II; Biosym Technologies, 1994). O2 was found to be the most negatively and O1 the least negatively charged O atom. The charge on O3 varies considerably with the molecular conformation and the relative position of F. Likewise we find that the charges are strongly influenced by the position of the H atoms. These results confirm that O1 is a poor acceptor, but the occurence of the different hydrogen-bonding motifs in the monofluoro-substituted mandelic acids cannot be rationalized from the calculated charges.

Table 4 illustrates the restriction on the combination of the two hydrogen bonds. The two H atoms capable of hydrogen bonding are never connected by intermolecular hydrogen bonds to the same acceptor (O2 or O3), except in **RM**, where H1 and H3 from molecule *A* are hydrogen bonded to O3*B*, but in this case H1 is involved in three-centre hydrogen bonds, the second acceptor being O2*B*. **RM** is the only structure showing three-centre hydrogen bonds where both hydrogen bonds are intermolecular.

Another interesting observation can be made from Table 4 concerning the differences in the packing of racemates and enantiomers. Hydrogen bonds between molecules related by glide planes are never formed in α-hydroxy acids. In contrast, the hydrogen-bonded chains between molecules of identical chirality (related by a twofold screw axis or translation) are the most common motif. The close proximity of the hydroxy and carboxyl groups is the likely reason for the lack of this motif, since it is formed in β-hydroxycarboxylic acids.

3.4. *Hydrogen-bonding patterns in the fluoromandelic acids*

Crystal packing in the optically active fluoro-substituted mandelic acids is illustrated in Figs. 2, 3 and 4. Fig. 5 shows schematic drawings of the hydrogen bonds in the corresponding racemic and optically active crystal structures.

The general motif found in the three crystal structures of optically active fluoromandelic acids is chains of rings that are linked together to form a sheet of rings.

p-Fluoromandelic acid forms hydrogen bonds between the same atoms in the racemate as in the optically active compound, illustrated by the schematic

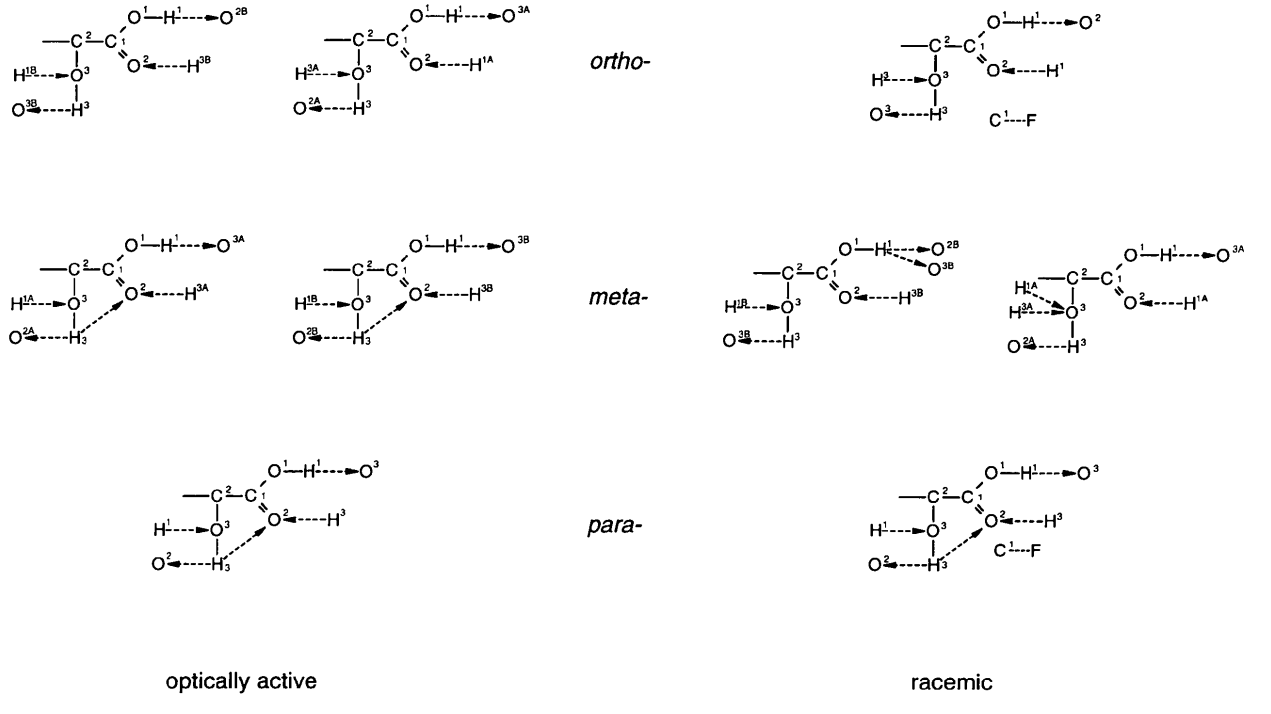

Fig. 5. Schematic drawing of the hydrogen-bonding scheme in racemic and optically active monofluoro-substituted mandelic acids.

drawings in Fig. 5. [The intramolecular hydrogen bond O3—H3···O2 was not listed by Larsen & Marthi (1994); O3···O2 2.7216 (7), H3···O2 2.441 (10) Å, O3—H3···O2 102.9 (8)°]. In both structures the intermolecular hydrogen bonds lead to the formation of sheets, but the significant difference between the O2—C1—C2—O3 torsion angle indicates that the structures are not similar. An analysis of the hydrogen-bonding patterns in terms of graph theoretical method (Bernstein, Davis, Shimoni & Chang, 1995; Etter, MacDonald & Bernstein, 1990) reveals the differences. With the highest priority motif being formed by the O1—H1···O3 and the second highest priority by the O3—H3···O2 hydrogen bond, the first-order network is $N_1 = R_2^2(10)C(5)$ for the racemate and $N_1 = C(5)C(5)$ for the optically active acid (Fig. 4).

OM and **OP** have very similar hydrogen-bond motifs. As mentioned previously, had the F substitution occurred on the same side of the molecule compared with the position of the hydroxy group for both molecules in **OM**, it would give rise to an unfavourably short F···F distance, corresponding to a repulsive interaction. The hydrogen-bonding pattern in **OM** appears less complex than that found in the metastable modification of the racemate. In **RM** the hydrogen bonds are formed between different atoms and between the crystallographically independent molecules; in addition, the three-centre hydrogen bonds further complicate the structure.

In **OO** the hydrogen bonds are formed between the same atoms as in **RM** if the O1*A*—H1*A*···O3*B* hydrogen bond in **RM** is ignored. However, the weaker interactions are formed between different atoms and the O—H···O hydrogen-bonding pattern is distinctly different. The O—H···O hydrogen-bonding pattern in **OO** is completely different from that observed in the racemate, which contains cyclic dimers interlinked by O3—H3···O3 hydrogen bonds.

3.5. *Thermodynamic properties*

The measured melting points listed in Table 6 agree well with the results reported by Collet & Jacques (1973), but the melting enthalpies of the optically active acids are *ca* 10% lower than the values reported previously. The binary phase diagrams for the three fluoromandelic acids are calculated (Jacques, Collet & Wilen, 1981) using the measured m.p.'s and enthalpies for the racemic and optically active acids listed in Table 6.

Assuming that the melts show ideal behaviour, the relative differences in melting enthalpies and entropies must be related to differences in the crystal structures.

The melting points for the optically active and racemic monofluoro-substituted mandelic acids are all in the range 362–426 K (Table 6) with associated melting enthalpies from 19 (**OO**) to 31 kJ mol^{-1} (**RO**). The melting enthalpy seems to depend on the number of molecules in the asymmetric unit. **OO**, **OM** and **RM**, which contain two molecules per asymmetric unit, have melting enthalpies close to 20 kJ mol^{-1}, whereas the melting enthalpies of *ca* 30 kJ mol^{-1} are observed for structures with one molecule per asymmetric unit. Since all the melting points are similar and close to 400 K, this will give rise to similar variations in the melting entropies.

Table 5. *Intra- and intermolecular interactions in the optically active monofluoro-substituted mandelic acids*

	$D\cdots A$ (Å)	D—H$\cdots A$ (°)	H$\cdots A$ (Å)
OO			
O1*A*—H1*A*···O2*B*^{i}	2.586 (1)	153 (2)	1.68 (3)
O1*B*—H1*B*···O3*A*	2.651 (1)	171 (2)	1.77 (2)
O3*A*—H3*A*···O3*B*^{ii}	2.726 (1)	172 (2)	1.87 (2)
O3*B*—H3*B*···O2*A*^{iii}	2.793 (2)	149 (2)	2.08 (2)
OM			
O1*A*—H1*A*···O3*A*^{iv}	2.612 (1)	162 (2)	1.81 (3)
O1*B*—H1*B*···O3*B*^{iv}	2.614 (1)	164 (2)	1.75 (3)
O3*A*—H3*A*···O2*A*	2.654 (1)	117 (2)	2.14 (3)
O3*A*—H3*A*···O2*A*^{v}	2.810 (2)	136 (2)	2.11 (2)
O3*B*—H3*B*···O2*B*	2.660 (1)	117 (2)	2.18 (3)
O3*B*—H3*B*···O2*B*^{vi}	2.813 (2)	139 (2)	2.14 (2)
OP			
O1—H1···O3^{vii}	2.618 (1)	167 (2)	1.79 (3)
O3—H3···O2	2.654 (1)	113 (2)	2.24 (3)
O3—H3···O2^{viii}	2.811 (1)	145 (3)	2.12 (2)

Symmetry codes: (i) $x+1, y, z$; (ii) $-x, y-\frac{1}{2}, 2-z$; (iii) $x-1, y, z$; (iv) $x, y-1, z$; (v) $1-x, y+\frac{1}{2}, 1-z$; (vi) $-x, y+\frac{1}{2}, 1-z$; (vii) $x, y+1, z$; (viii) $\frac{3}{2}-x, y-\frac{1}{2}, 1-z$.

It is noteworthy that the very different appearances of the phase diagrams in Fig. 6 can be caused by small differences in the enthalpy and entropy for the racemic and enantiomeric crystals. We will attempt to relate these small differences to differences in the intermolecular interactions and molecular conformations in the six crystals structures.

OP and **OM** are isostructural if one neglects the substitution of F atoms. Melting of these two compounds requires breaking of an identical system of hydrogen bonds. In **OM** one of the independent molecules is in an unsual conformation that may have a slightly higher energy than the other molecules in **OM** and **RM**, which could be reflected in the differences in melting enthalpy between **OM** and **OP** of *ca* 5 kJ mol^{-1}.

Each pair of racemic and enantiomeric compounds shows pronounced differences. *ortho*-Fluoromandelic acid is the only acid which behaves 'normally' by forming a racemic compound that is higher melting than the pure enantiomer. It contains two independent molecules in the crystals of the pure enantiomer and one in its racemic compound. The hydrogen-bonding schemes in the two compounds are so different that we relate the difference in melting enthalpies to the difference in hydrogen-bond interactions.

The structures of racemic and enantiomeric *meta*-fluoromandelic acids are similar with respect to their hydrogen-bond patterns and the two compounds show

Table 6. *Thermochemical data for the racemic and optically active monofluoro-substituted mandelic acids**

	OO	RO	OM	RM	OP	RP
m.p.	361.8 (5)	388.3 (5)	394.2 (5)	368.4 (5)	425.8 (5)	408.9 (5)
ΔH^{θ}_{fus} (kJ mol^{-1})	19.1 (5)	31 (2)	22.3 (5)	21 (2)	27.2 (8)	30 (2)
ΔS^{θ}_{fus} (J mol^{-1} K^{-1})	53 (1)	79 (2)	57 (1)	57 (2)	64 (2)	73 (2)
No. of independent molecules	2	1	2	2	1	1

* Data for the racemic monofluoro-substituted mandelic acids are taken from Larsen & Marthi (1994).

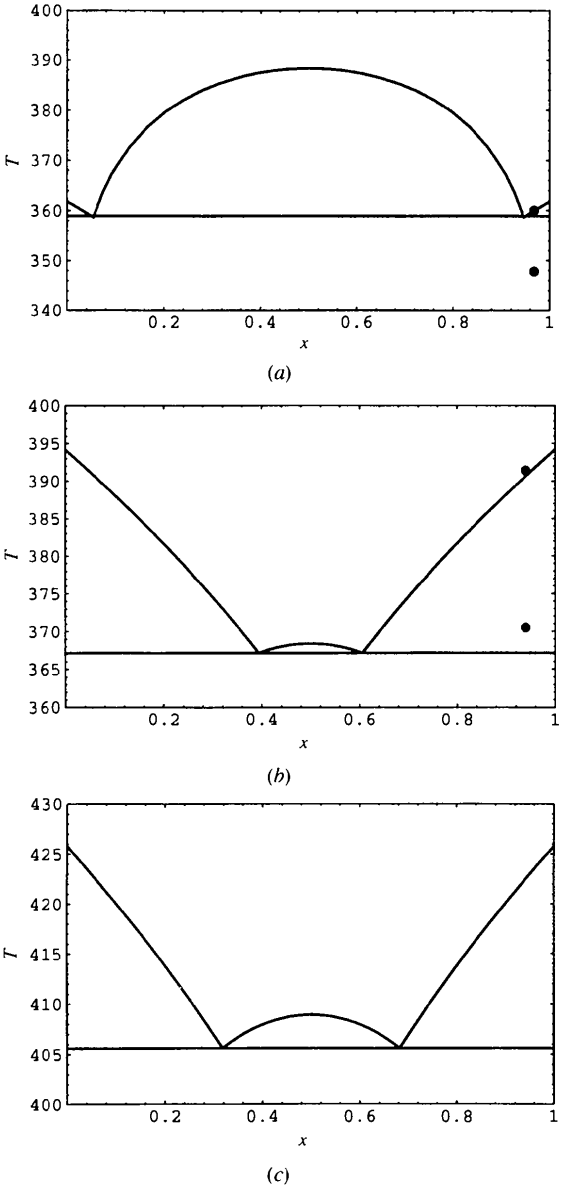

Fig. 6. Phase diagrams for (*a*) *ortho*-, (*b*) *meta*- and (*c*) *para*-fluoromandelic acids. The dots mark the peak temperatures for the eutectic and final melting peaks for samples with known enantiomeric composition determined by optical rotation.

almost identical melting entropies and enthalpies. The formation of racemic compounds is favoured by the term $TR\ln 2$ arising from the entropy of mixing (Jacques, Collet & Wilen, 1981) and the existence of a racemic compound of *meta*-fluoromandelic acid appears to depend largely on this $TR\ln 2$ term.

Both forms of *para*-fluoromandelic acid crystallize with one independent molecule per asymmetric unit. The hydrogen bonds are remarkably alike and the carbon–fluorine interactions which only take place in the racemic acid can explain the small difference in the melting enthalpies, which leads to the formation of the racemic *para*-fluoromandelic acid.

The above analysis has shown that the different appearence of the binary phase diagrams for the enantiomeric forms of the monofluoro-substituted mandelic acids can be rationalized in terms of the small differences in intermolecular interactions in the crystals. This makes it difficult (or impossible) to formulate very general rules that relate crystal structures to thermochemical properties. However, systematic studies such as that conducted here are needed to improve the understanding of the relations between structure and thermochemical properties of chiral systems.

This research was supported by the Danish Natural Science Research Council by a grant to SL. We thank the Faculty of Science, University of Copenhagen, for economical support to KM and Mr F. Hansen for assistance in the experimental crystallographic work. The help and assistance from Dr E. J. Pedersen and Professor E. Larsen with the NMR measurements and preparations are gratefully acknowledged. The thermoanalytical equipment was made available through a grant from the Lundbeck Foundation.

References

Allen, F. H., Bellard, S., Brice, M. D., Cartwright, B. A., Doubleday, A., Higgs, H., Hummelink, T., Hummelink-Peters, B. G., Kennard, O., Motherwell, W. D. S., Rodgers, J. R. & Watson, D. G. (1979). *Acta Cryst.* B**35**, 2331–2339.

Bernstein, J., Davis, R. E., Shimoni, L. & Chang, N.-L. (1995). *Angew. Chem.* **34**, 1555–1573.

Bernstein, J., Etter, M. & Leiserowitz, L. (1994). *Structure Correlation*, edited by H.-B. Bürgi & J. Dunitz, pp. 431–507. Weinheim: VCH.
Blessing, R. H. (1987). *Cryst. Rev.* **1**, 3–58.
Biosym Technologies (1994). *InsightII Reference Guide*. Version 2.3.0. Biosym Technologies, San Diego, USA.
Biosym Technologies (1995). *Cerius*^{2}. *Installation and Administration Guide*. Release 2.0. Biosym Technologies, San Diego, USA.
Cesario, M., Guilhem, J., Pascard, C., Collet, A. & Jacques, J. (1978). *Nouv. J. Chim.* **2**, 343–349.
Collet, A. & Jacques, J. (1973). *Bull. Soc. Chim. Fr.* pp. 3330–3334.
Etter, M. (1991). *J. Phys. Chem.* **95**, 4601–4610.
Etter, M., MacDonald, J. C. & Bernstein, J. (1990). *Acta Cryst.* B**46**, 256–262.
Flack, H. D. (1983). *Acta Cryst.* A**39**, 876–881.
Flack, H. D. & Schwarzenbach, D. (1988). *Acta Cryst.* A**44**, 499–506.
Jacques, J., Collet, A. & Wilen, S. H. (1981). *Enantiomers, Racemates, and Resolutions*, pp. 94–95, 131–135. New York: Wiley.
Johnson, C. K. (1976). *ORTEP*II. Report ORNL-5138. Oak Ridge National Laboratory, Tennessee, USA.
Korver, O. (1970). *Tetrahedron*, **26**, 5507–5518.
Korver, O., De Jong, S. & van Soest, T. C. (1976). *Tetrahedron*, **32**, 1225–1229.
Larsen, S. & Marthi, K. (1994). *Acta Cryst.* B**50**, 373–381.
Larsen, S. & Marthi, K. (1995). *Acta Cryst.* B**51**, 338–346.
Leiserowitz, L. (1976). *Acta Cryst.* B**32**, 775–802.
Patil, A. O., Pennington, W. T., Paul, I. C., Curtin, D. Y. & Dykstra, C. E. (1987). *J. Am. Chem. Soc.* **109**, 1529–1535.
Sheldrick, G. M. (1990). *Acta Cryst.* A**46**, 467–473.
Sheldrick, G. M. (1993). *SHELXL*93. *Program for the Refinement of Crystal Structures*. University of Göttingen, Germany.
Spek, A. L. (1990). *Acta Cryst.* A**46**, C34.